MHD Simulation of Resonant Magnetic Perturbations

H.R. Strauss[1] L. Sugiyama[2], G.Y. Park[1], C. S. Chang[1], S. Ku[1] I. Joseph[3]
[1]New York University, New York, New York, USA 10012
[2] MIT, Cambridge, MA, USA 02139
[3]University of California, San Diego, CA, USA 92186
strauss@cims.nyu.edu

Abstract Resonant magnetic perturbations (RMP) have been found effective in suppressing ELMs in the DIII-D experiment [1, 2] Simulations with the M3D code indicate that plasma rotation has an essential effect on the RMP. When rotation is below a threshold, the RMP magnetic field is amplified above the vacuum field, and acquires a helical structure. The magnetic field is stochastic in the outer part of the plasma, causing temperature and density loss. At higher rotation speed, the stochastic layer is thinner. The temperature is similar to the initial non rotating unperturbed state. Rotation and the screened RMP cause a density loss which extends into the plasma core.

I. Introduction

Resonant magnetic perturbations (RMP) have been found effective in suppressing ELMs in the DIII-D experiment[1, 2]. The RMP is produced by external coils producing a magnetic perturbation with toroidal mode number $n = 3$. The vacuum magnetic perturbation causes the magnetic field to become stochastic in the outer $1/3$ of the plasma. It would be expected that this would cause a large temperature and density loss where the magnetic field is stochastic. Instead the density gradient is reduced in the edge region, accompanied by a large density pumpout in the core, while the temperature is not strongly affected. The reduced pressure gradient stabilizes the peeling ballooning modes which appear to cause ELMs. It is thought that the plasma rotation screens the RMP from the plasma, producing a thin stochastic magnetic field region at the plasma edge. If so, then the density pumpout in the core must be explained. Simulations with the M3D code[3] show that MHD effects have some features of the experimental observations. In the absence of toroidal rotation, the RMP is amplified, acquiring a helical structure. There is a loss of temperature and density in the stochastic magnetic field region. Plasma rotation reduces the width of the stochastic magnetic field layer. The temperature loss is confined to the edge, while the density loss extends into the plasma core. However, the density pumpout observed experimentally [1] is much larger than the MHD pumpout effect. In future work, the MHD simulations will be supplemented with kinetic modeling with the XGC [4] gyrokinetic code.

II. Numerical MHD Simulations

Simulations with the M3D code [3] indicate that plasma rotation has an essential effect on the RMP, both on temperature and density. The simulations were done starting from an EFIT DIII-D equilibrium reconstruction, g126006, which was made ELM stable by application of an RMP produced by the external I coil, with toroidal period $n = 3$. The magnetic perturbations were calculated by Biot Savart calculation of the field from the coil current. The initial equilibrium is shown in Fig.1. The equilibrium poloidal flux ψ is shown in Fig.1(a), the temperature in Fig.1(b), the density in Fig.1(c), and the vacuum RMP magnetic poloidal magnetic flux, ψ_{RMP}, which varies toroidally as $\sin(3\phi)$ is shown in Fig.1(d).

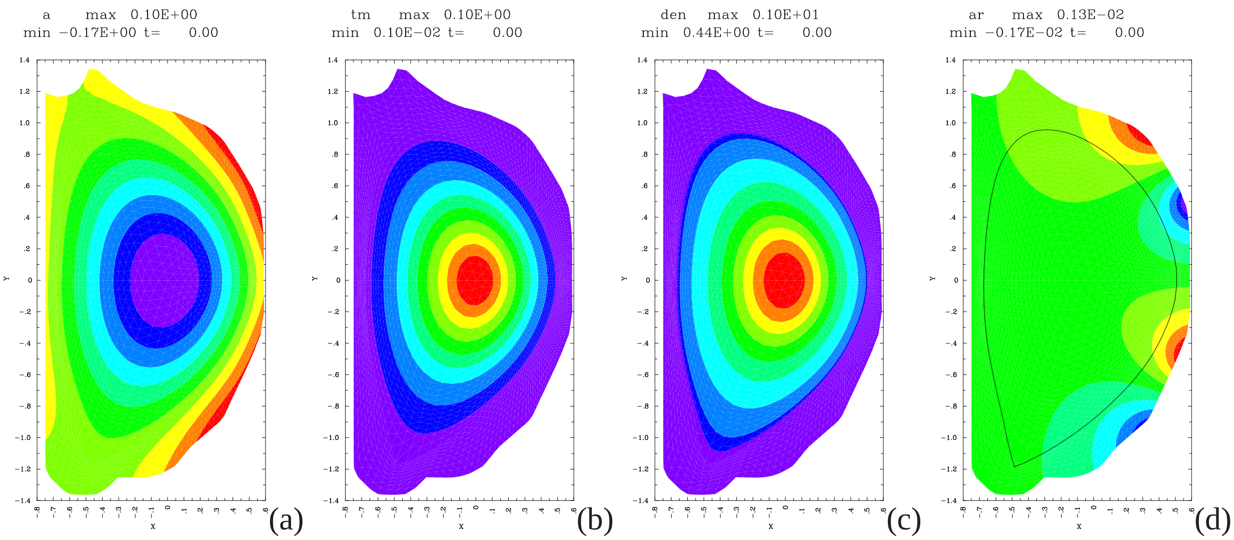

Figure 1: (a) initial magnetic flux contours of DIII-D equilibrium reconstruction g126006. (b) initial temperature contours in the equilibrium reconstruction (c) initial density contours. (d) initial RMP perturbation ψ.

First consider the case in which the RMP is applied, without rotation. This is what would have been predicted to occur, before the RMP experiments were performed. The vacuum RMP is included in the initial state shown in Fig.1(d). Because of the RMP, the initial state is not in equilibrium. The vacuum RMP produces a broad stochastic magnetic field layer, in approximately the outer third of the plasma. The initial state is evolved to time $t = 87\tau_A$, where $\tau_A = R/v_A$ is the toroidal Alfvén time, where R is the major radius and v_A is the Alfvén speed. The Lundquist number on axis is $S = 10^6$, which must be lower than experiment for numerical reasons. The resistivity varies as $T^{-3/2}$ self consistently, where T is the temperature. At the bottom of the pedestal, $S = 10^4$.

The temperature is shown in Fig.2(a). As expected, there is a large cooling effect in the outer plasma where the magnetic field is stochastic. This is what the RMP would have been expected to do *a priori* because of parallel thermal transport in the stochastic magnetic field. The density is shown in Fig.2(b). The density evolves on a slower time scale than the temperature Density is lost in the outer plasma region, like the temperature. The density and pressure will eventually relax to a new equilibrium, with nonzero gradients only inside the stochastic layer, where there are closed magnetic flux surfaces.

The RMP perturbation is shown Fig.2(c). It can be seen that the RMP field is amplified by the plasma response. It extends further into the plasma and acquires a $\cos(3\phi)$ component, with a helical, ballooning like structure.

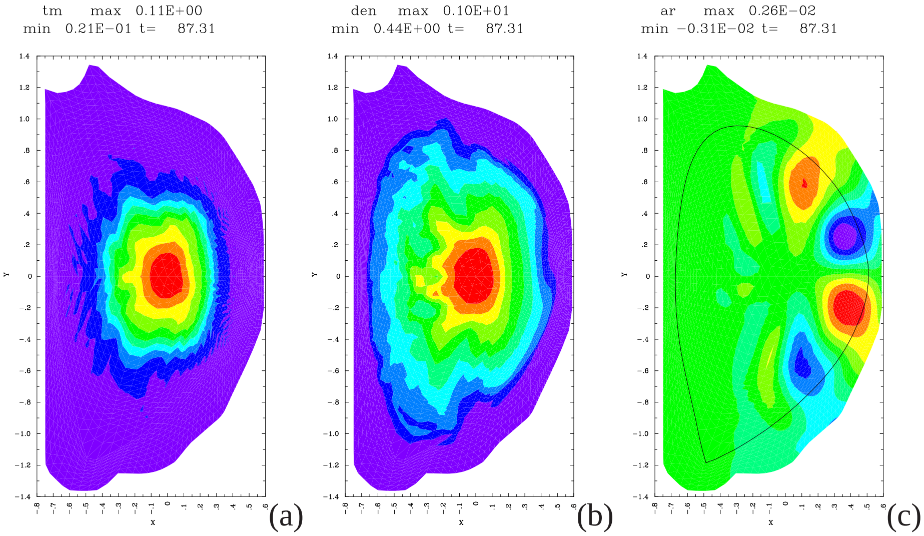

Figure 2: (a) temperature in the nonrotating RMP case at $t = 87\tau_A$. There is a large cooling effect in the outer plasma layer where the magnetic field is stochastic. This is what the RMP would have been expected to do. (b) density in the nonrotating RMP case at $t = 87\tau_A$. There is a large edge density loss. (c) RMP ψ at $t = 87\tau_A$. The RMP is amplified and couples to a helical structure containing $\sin(3\phi), \cos(3\phi)$ components.

III. Magnetic Screening

The perturbed poloidal flux ψ is quite different in the presence of rotation. The applied flux is shown in Fig.1(d). In the case of no rotation, the RMP flux increases in the plasma, in Fig.2(c). With rotation, the initial flux is excluded from the plasma, depending on the rotation and plasma resistivity.

The growth of the poloidal flux perturbation in the absence of rotation can measured from the maximum amplitude of the $n = 3$ magnetic flux ψ in a plane $\phi = 0$, out of phase with the applied RMP, at a fixed time after applying the RMP. Measuring the out of plane $\cos(3\phi)$ perturbation allows a clean separation from the applied RMP, which is proportional to $\sin(3\phi)$. The results, shown in Fig.3(a) indicate a scaling with resistivity as $S^{-1/2}$. The out of plane growth of the perturbation has a Sweet Parker magnetic reconnection scaling. The critical rotation required to prevent the growth of the perturbations, is evidently adequate to to screen the RMP itself from the plasma and heal the stochastic magnetic field. In turn this causes the temperature to be well confined. This suggests a critical scaling of rotation as $S^{-1/2}$.

The modification of ψ_{RMP} by rotation is seen in Fig.3(b). This a plot of ψ_{RMP} in the plane $\phi = \pi/6$, where the $\cos(3\phi)$ dependence of the RMP is maximum. The abscissa is the distance along a ray from the magnetic axis to a point on the boundary where ψ_{RMP} is a maximum. The solid curve is the applied RMP. The dashed curve is the perturbed flux along the same ray, with rotation.

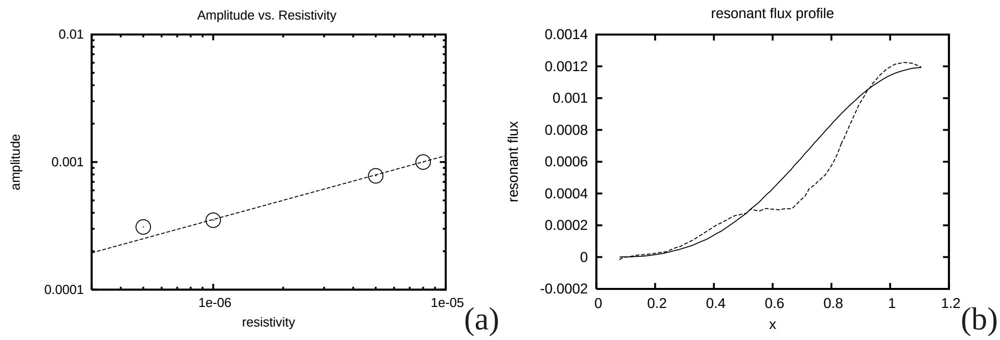

Figure 3: (a) amplitude of enhanced magnetic flux as a function of resistivity η, with fit to $\eta^{1/2}$. (b) Profile plot of perturbed flux with rotation at $t = 0, 52\tau_A$. The profile is taken along a ray from the magnetic axis to the boundary, where ψ_{RMP} is a maximum. The rotation reduces the amplitude of the perturbed flux in the plasma.

It can be seen that the perturbation is reduced by the rotation, although not completely screened from the plasma. The rotation profile is broad, taken from the equilibrium reconstruction data. The magnitude of the rotation was increased to compensate for the artificially low S value, to a peak value of toroidal velocity $v_\phi = 0.075 v_A$. The experimental peak toroidal velocity is about an order of magnitude lower, consistent with the maximum S being two orders higher in the experiment. In ITER, the toroidal rotation is expected to be an order of magnitude less than in DIII-D, but S will again be two orders higher, so that the screening of RMP should occur in ITER [5]. There is still a concern that the non resonant part of the RMP, which would not be expected to experience screening, might damp the toroidal rotation. Then, the poloidal rotation would have to provide screening.

IV. Rotation and Density Loss

Plasma rotation has several effects on the density and temperature. The most important effect is that the stochastic magnetic field layer is narrower, because the RMP is screened by rotation. The effects of the case without rotation now occur in a narrower layer near the magnetic separatrix. In the stochastic layer, the temperature is rapidly cooled, followed by density loss on a slower sound wave time scale.

Rotation also modifies the MHD equilibrium [6, 7], even without the RMP. It causes the surfaces of constant density and pressure to deviate from the magnetic surfaces. The temperature is a flux function, because of high parallel thermal conduction. In the simulations in Fig.4, the toroidal velocity function is taken from the equilibrium reconstruction. It is peaked on axis, and zero outside the magnetic separatrix.

The deviation of the density from being constant on flux surfaces is proportional to the inverse aspect ratio, and the ratio of the velocity to the sound speed squared. In the experiments, the aspect ratio is rather low and the parallel and/or toroidal velocity is a fraction of the sound speed. The toroidal rotation causes an outboard shift of the density surfaces, which can evidently cause density to leak onto open field lines.

When the RMP is applied, the density loss is enhanced. The rotation velocity was increased for numerical reasons, to give sufficient screening near the separatrix, to a maximum value (on axis) $v_\phi = 0.075 v_A$. Starting from profiles in the eqdsk file g126006, the equilibrium was evolved until $t = 72\tau_A$. At this point the evolution was continued, both with and without an applied RMP, until $t = 127\tau_A$. The density without the RMP is shown if Fig.4(a), and the with the RMP is shown in Fig.4(b). Comparing the density contours, it can be seen that the RMP produces a shrinkage of the density. The lost density is spun off in a blob which accumulates in a low magnetic field region near the top of Fig.4(a),(b). The density profile as a function of $R - R_0$, in the midplane $Z = 0$ at $t = 127\tau_A$, without the RMP, is shown in Fig.5(a) (solid line). The density profile with the RMP turned on is shown in Fig.5(a)(dashed line). The density loss is largest at the edge, but extends to the plasma core. If the initial density profile is more peaked, the central density loss can be substantial. The temperature in the same case, at the same times, is shown in Fig.4(c),(d). The temperature with rotation but without the RMP is shown in Fig.4(c). The addition of the RMP, in Fig.4(d), causes the temperature to cool and contract, because of a thin stochastic layer inside the original separatrix. The density and temperature respond differently to the presence of the stochastic layer. The density is spun off, while the temperature rapidly cools because of thermal conduction along the magnetic field lines. The temperature profiles are compared in Fig.5(b), without the RMP (solid line) and with the RMP. The temperature perturbation is localized to the edge. The temperature gradient is reduced at the separatrix, but increases slightly further in.

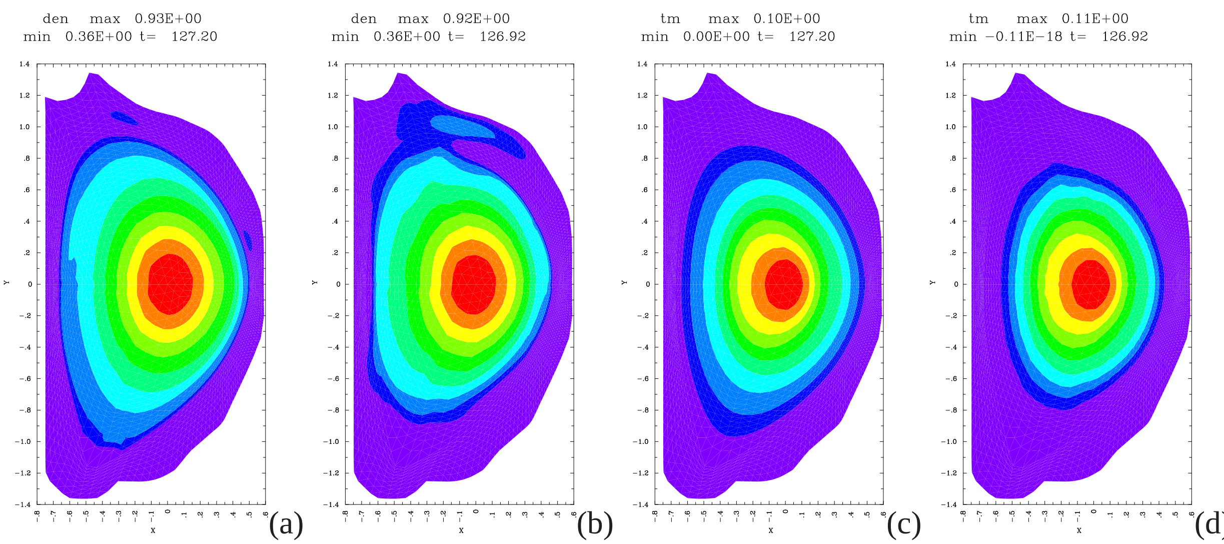

Figure 4: (a) density at time $t = 127\tau_A$ in the rotating case with no RMP. There is density loss because of the rotating equilibrium effect. (b) density at time $t = 127\tau_A$ in the rotating case with RMP. The density loss is enhanced by the RMP. (c) temperature at time $t = 127\tau_A$ in the rotating case with no RMP. (d) temperature at time $t = 127\tau_A$ with rotation and RMP.

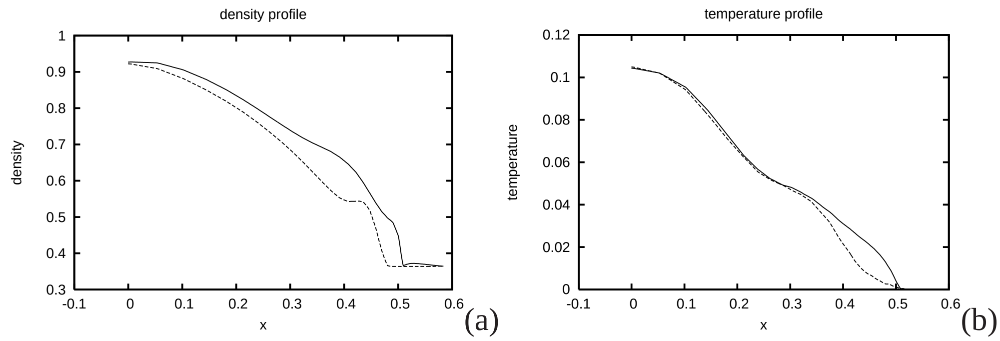

Figure 5: (a) density profiles for the previous cases. The solid line is from Fig.4(a), and the dashed curve is from Fig.4(b). There is some loss of density, which extends to the center of the plasma. (b) temperature profiles as a function of $R - R_0$ at $Z = 0$ for the previous cases Fig.4(c),(d). The temperature loss penetrates less into the plasma, and part of the outer temperature gradient is steepened.

Poloidal rotation has a large effect on the density. In fact there can be a density discontinuity and possibly shocks at the magnetic surface where the flow is transonic [8]. There will always be a transonic magnetic surface if the poloidal flow is nonzero at the magnetic separatrix, where the poloidal sound frequency $c_s/(qR)$ must vanish. In that case, the flow is supersonic at the separatrix and becomes subsonic inside the plasma. It is numerically problematic dealing with the shocks, which are enhanced by the need to use higher flow speeds than in experiment, in order to screen the magnetic field. Development of a free boundary Grad Shafranov solver with flow is in progress, to help separate the effects of flow from the effects of the RMP.

In future work, the radial electric field will be obtained from simulations using the XGC [4] edge kinetic neoclassical code.

There is a resemblance between RMP and ELMs. Both relax the pressure profile at the edge. In both cases, the temperature profile change is localized to the separatrix, but the density profile change is larger and extends to the plasma core. This is seen by comparing the RMP density profiles in Fig.5(a) with ELM density profiles in Fig.6(a), which shows profiles at several different times during an ELM crash of the unstable DIII-D equilibrium g113207. Evidently this is a plasma decompression due to pressure loss at the edge. The temperature is much less affected, comparing Fig.5(b) with Fig.6(b). Although the density perturbations extend to the core, and can be rather large for a peaked density profile, MHD can only partially explain the large density pumpout observed in DIII-D. Other kinetic effects that might explain the pumpout are being investigated using XGC [4].

V. Conclusions

Numerical simulation with the M3D nonlinear MHD code verifies that plasma toroidal rotation can screen an RMP magnetic field from the plasma, reducing the width of the stochastic magnetic layer and reducing parallel thermal conduction. Poloidal and toroidal rotation can also cause density loss. When the rotation is small, the RMP can be amplified and acquire a component aligned with the magnetic field, similar to a ballooning mode. This

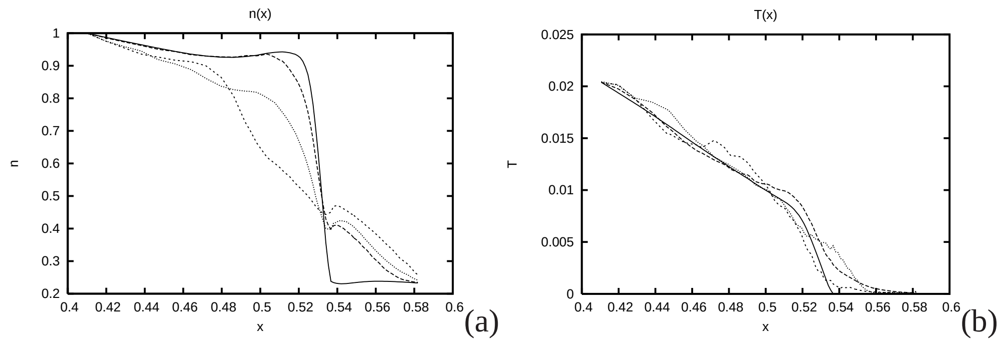

Figure 6: (a) density profiles in an ELM, at different times, as a function of $R - R_0$ at $Z = 0$. The solid line is the initial density, which relaxes to a lower gradient. The density perturbation extends to the plasma core. (b) temperature profiles for the same case. The temperature perturbation penetrates much less into the plasma than the density perturbation.

component grows as $S^{1/2}$, and can extend deep into the plasma. Plasma rotation sufficient to prevent amplification is also adequate to screen the RMP from the plasma. Rotation and the screened RMP cause a density loss which extends into the plasma core, but is small compared to the density pumpout observed in DIII-D [1]. The results suggest that RMP screening should be effective in a high temperature experiment such as ITER.

Acknowledgments

This work was supported by the U.S.D.O.E.

References

[1] EVANS, T. E., K. H. BURRELL, K. H., FENSTERMACHER, M. E., MOYER, R. A., OSBORNE, T. H., SCHAFFER, M. J., WEST, W. P., YAN, L. W., BOEDO, J. A., DOYLE, E. J., JACKSON, G. L., JOSEPH, I., LASNIER, C. J., LEONARD, A. W., RHODES, T. L., THOMAS, P. R., WATKINS, J. G., ZENG, L., The physics of edge resonant magnetic perturbations in hot tokamak plasmas, Phys. Plasmas **13** (2006) 056121.

[2] MOYER, R. A. EVANS, T. E., OSBORNE, T. H., THOMAS, P. R., BECOULET, M., HARRIS, J., FINKEN, K. - H., BOEDO, J. A., DOYLE, E. J., FENSTERMACHER, M. E.,GOHIL, P., GROEBNER, R. J.,GROTH, M., JACKSON, G. L., LAHAYE, R. J., LASNIER, C. J., LEONARD, A. W., MCKEE, G. R., REIMERDES, H. RHODES, T. L., RUDAKOV, D. L., SCHAFFER, M. J., SNYDER, P. B., WADE, M. R., WANG, G., WATKINS, J. G., WEST, W. P., ZENG, L., Edge localized mode control with an edge resonant magnetic perturbation, Phys. Plasmas **12** (2005) 056119.

[3] PARK, W., BELOVA, E.V., FU, G.Y., TANG, X.Z., STRAUSS, H.R., SUGIYAMA, L.E., Plasma Simulation Studies using Multilevel Physics Models, Phys. Plasmas **6**, (1999) 1796.

[4] CHANG, C. S., KU, S., WEITZNER, H., Phys. Plasmas **11** (2004) 2649.

[5] BECOULET, M., NARDON, E., HUYSMANS, G., ZWINGMANN, W., THOMAS, P., LIPA, M., MOYER, R., EVANS, T., CHUYANOV, V., GRIBOV, Y., POLEVOI, A., VAYAKIS, G., FEDERICI, G., SAIBENE, G., PORTONE, A., LOARTE, A., DOEBERT, C., GIMBLETT, C., HASTIE, J., PARAIL, V., Numerical study of the resonant magnetic perturbations for Type I edge localized modes control in ITER, Nucl. Fusion **48**, (2008) 024003.

[6] STRAUSS, H. R., Toroidal magnetohydrodynamic equilibrium with toroidal flow, Phys. Fluids **16** (1973) 1377.

[7] HAMEIRI, E., The equilibrium and stability of rotating plasmas, Phys. Fluids **26** (1982) 230.

[8] BETTI, R., FRIEDBERG, J. P., Radial discontinuities in tokamak magnetohydrodynamic equilibria with poloidal flow, Phys. Plasmas **7** (2000) 2439; GUAZZOTTO, L., BETTI, R., MANICKAM, J., KAYE, S., Numerical study of tokamak equilibria with arbitrary flow, Phys. Plasmas **11** (2004) 604.